06

Quantum-mechanical simultion of the Fe-Si(001) system at the growth stage of a solid wetting layer

© V.G. Zavodinsky,[1] N.I. Plyusnin,[2] O.A. Gorkusha[1]

[1] Khabarovsk Branch of the Institute of Applied Mathematics of FEB RAS,
680000 Khabarovsk, Russia
[2] Budyonny Military Academy of the Signal Corps,
194064 St. Petersburg, Russia
e-mail: plusnin@dvo.ru

Within the framework of density functional theory and the pseudo-potential method, the atomic and electronic structures of the film-substrate system at 0 K in the state of minimum free energy were studied during step-by-step (with a step size of one atomic diameter of Fe) deposition of a Solid Wetting Layer (SWL) Fe up to a thickness of 8 monolayers (ML) onto a normal Si(001) lattice compressed by 1.33 times in the $\langle 011 \rangle$ direction. It is shown that SWL grows in three stages: first, 2D, i.e. SWL with compositions Fe_2Si and $FeSi$ is formed on a normal and, accordingly, compressed substrate, and then 2D-SWL Fe and 3D-SWL Fe are sequentially formed. During the growth process of SWL, a three-dimensional environment of Fe atoms is built and the degree of coordination of Fe atoms, with a Fe thickness of 6.4 ML, reaches 10. As a result of this, an electronic structure specific of the bulk phase (BP) Fe is formed. After which, at a thickness of 8 ML Fe, a metastable and stable BP Fe is formed with an *bc* monoclinic lattice and, accordingly, *bcc*, i.e. lattice on a normal and compressed substrate. This process is accompanied by compaction of adjacent layers of the Si substrate and their transformation into high-pressure phases.

Keywords: solid wetting layer, atomic coordination, electronic states, Fe-Si(001), simulating.

Introduction

In the early 1980s, there was an upsurge in interest in studying the formation and electronic structure of ultrathin metal films on silicon, associated with the increasing use of metal contacts on silicon and with the spread of ultra-high vacuum methods of electronic (and other types) spectroscopy of surfaces and thin films. This upsurge in interest continued until the advent of scanning probe microscopes and led to the accumulation of a huge array of results, in particular data from electron spectroscopy with a synchrotron X-ray source (see, for example, [1,2]). After which, the vector of research changed to nano-objects that are visually visible at the atomic level: clusters, fullerenes, nanotubes, etc. (see, for example, the bibliography of J.H. Weaver [3]).

This huge array of information in its interpretation was based on traditional theories and models of film growth, which continue to be used to this day (see, for example, [4]). But these theories, as a rule, relate to equilibrium conditions or conditions close to them, do not take into account all factors, and are very far from being adequate in the event of a violation of equilibrium conditions. For real conditions, it is necessary to have more accurate growth models, in particular, models that take into account the formation of a solid wetting layer (SWL), which adapts in structure to the substrate [5,6] in the process of deposition from hot vapor and freezing by a cold substrate to solid aggregative state.

For example, the traditional capillary theory of film growth [7] provides for mass transfer in the form of diffusion and/or spreading over the surface or inside the film. In contrast to this, SWL, which usually precedes the growth of the bulk phase of the film, is frozen to a solid aggregative state and there is no such mass transfer in it. Therefore, the SWL forming model should be different. In addition, the question arises: what mechanism of SWL forming gives rise to the nucleation of the bulk phase (BP) in SWL when atoms are added to the SWL surface from the outside and when its thickness increases?

It is obvious that, due to changes in the degree of adaptation of SWL to the substrate, as the thickness increases, its density, structure and stress state change. In this case, a change in the atomic environment in SWL changes the forces of electronic interaction, and they, in turn, further rearrange the atomic environment, etc., until a spontaneous transition to BP occurs. In addition, during the transition to BP, latent thermal energy is released, which activates inter-diffusion, formation of a junction at the interface with the substrate and causes agglomeration of the film into islands.

For the first time, a hypothesis about the mechanism of initiation of the transition of SWL to BP of a metal, caused by the formation of a collective electronic interaction of atoms at a threshold thickness, a change in atomic density, the accumulation of stresses in the film, their relaxation and,

as a result, the activation of mixing of the metal with silicon, was proposed in 1984, while studying plasmonic losses during the growth of several Cr monolayers on Si(111) and SiO_x [8,9]. A later (1986 g.) formulation by V.K. Adamchuk, I.V. Lyubinetsky and A.M. Shikin, based on a study of the growth of noble metals on silicon [10], emphasized the role transition of electronic interaction to collective interaction, but did not consider all these processes. Their formulation was that the basis of „...the mixing...are effects...due to the hybridization of *d*-electrons of a metal with *sp*-electrons of a semiconductor... during the transition from isolated atoms to a structure characteristic of a solid" (i.e. during the transition to the collective interaction of atoms). At the same time, they noted that the differences in the valence *d* bands of various transition metals lead to different degrees of hybridization with the*sp* bands of silicon and to their varying degrees of mixing at the interface.

Indeed, the role of the collective interaction of atoms in changing the density of electronic bands at the metal-semiconductor (silicon) interface and the exchange-correlation potential at this boundary was known earlier [11–13]. But the fact that this interaction manifests itself in a change in the spatial electronic and atomic density, as well as in the creation of stresses in a thin film of metal on silicon, at it thickness of several monolayers, and that this leads to mixing of the metal with silicon was unexpected, and was not predicted by theory and had no previous explanation.

The above-mentioned hypothesis was prompted by the idea of plasmons in a thin film as a result of the collective interaction of electrons in the valence sub-bands, as well as the dependence of the plasmon energy on the film density. The identical nature of changes in the intensity and energy of these plasmons with increasing thickness in the Cr film, as well as threshold (after several monolayers) mixing on Si(111) and agglomeration on SiO_x indicated that the formation of a bulk electronic structure is the cause of both mixing and agglomeration and that this process changes the density and stress in the film to a critical value at which these processes occur.

But a systematic study of the growth of SWL of the transition 3*d* metal on silicon was required, since in the literature the conditions for the growth of metal on silicon, which influenced the mechanism of mixing SWL with silicon, were ambiguous and uncertain. To prove the point conclusively for the hypothesis, repeatable (under identical conditions) and ideal conditions for metal growth on silicon (without thermally activated diffusion) were required. In addition, it was necessary to generalize (taking into account SWL) to other transition 3*d* metals on silicon [5]. All these problems were purposefully solved by N.I. Plyusnin and his team of staff members (see, for example, references in the works [14,15]).

This work provides a study for first-principles study of metal SWL growth on silicon and its transition to BP, which develops the above-mentioned hypothesis and shows that increasing the SWL thickness changes the atomic coordination, and this, in turn, changes the electronic structure of the SWL valence bands.

1. Growth of SWL and its transition to BP

Here we consider the evolution of SWL Fe frozen at $0\,K$ on Si(001) after instantaneous deposition of layers Fe. In this case, the Fe layers consist of atomic chains that lie in potentially advantageous positions & mdash; the upper rows of interstices on the surface of the growing layer.

At each deposition step, a layer of atomic chains Fe with a total thickness of one atomic diameter ($1\,a.d. = 1.6\,ML$) is added. Moreover, after each deposition step, the system, due to electronic interaction in the SWL itself and between the SWL and the substrate, freely evolves over the required amount of time into a state with a minimum of free energy. Ultimately, at a certain thickness of the SWL, its vertical size is reached, equal to the Minimum Critical Thickness (MCT), at which a three-dimensional cluster,i.e.a nucleus of several atoms, is formed, and after which the transition from SWL to BP occurs.

In the absence of lattice coherence of the adsorbate (Fe) and the substrate (Si) under freezing conditions and for an ideally smooth (001) for surface of the substrate, it is most likely that the MCT value lies between two ML and two atomic diameters (a.d.). Thus, the MCT value can be in the range from 2 to $3.2\,ML$ (taking into account the fact that $1\,a.d. = 1.6\,ML$).

At the same time, the electronic influence of the substrate and vacuum on the SWL will begin to disappear when the SWL thickness exceeds two valence electron screening lengths. This screening length in a metal with its dense packing is approximately equal to $1\,a.d.$ Therefore, this factor will work after the formation of a volumetric environment in SWL, and the MCT interval may exceed $3.2\,ML$. This increase in the MCT thickness (up to $4\,ML$ and more) is consistent with the conclusion made in the work [16] that „...if ... the structure of the first monolayer differs noticeably from the structure of its own volume, then three-dimensional growth can begin above the first monolayer, and the film will grow in the Stranski-Krastanov growth mode. The onset of this growth mode may be delayed by several monolayers due to long distance exposure to the substrate...".

If the adsorption of atoms on the substrate does not occur under freezing conditions and the surface of the substrate is not atomically smooth (rearranged, disordered, has stacking faults, steps, etc.), then the range of SWL formation can begin from fractions of ML.

For example, the surface of the Si(111)7×7 structure with a size of 49 atoms consists of alternating un-fault and fault cells, each of which contains 6 Si adatoms. In cells„un-fault", the packing of atoms is normal (ABC type) and less dense as in Si(111). And in cells „fault" it is defective (AB) and more dense. Therefore, the adsorption of metal atoms is more likely to occur in cells „fault", or adsorption will occur by replacing Si adatoms with metal

atoms in cells „un-fault" and „fault". In this case, due to surface diffusion (if there is sufficient heating), these cells will be uniformly filled with the adsorbant, which will lead to the formation of so-called magic clusters, ordered into the structure 7×7 [17,18], during submonolayer coatings.

On the other hand, when there is a correspondence (at least super-structural one) between the lattices of the adsorbate ad the substrate, then, despite their heterogeneity, a case is possible when the SWL will be epitaxially stabilized to a thickness greater than 4 ML. Thus, under conditions of moderate heating of the substrate by a flow of metal atoms, the deposition of metal onto silicon will lead to its mixing with the substrate and the formation of SWL of a silicide composition. This SWL can even grow epitaxially if in the metal-silicon system there is a bulk silicide of similar composition that grows epitaxially on silicon.

An example is SWL Cr with super-structural conjugation $(\sqrt{3} \times \sqrt{3})$-$R30°$, which is formed in the Cr-Si(111) system when several monolayers are deposited on a moderately heated substrate [19,20]. This occurs because in the Cr-Si(111) system, epitaxial growth of bulk silicide CrSi [21] is observed. It is interesting that in the same system, when Cr is deposited onto Si(111)7×7 substrate heated to 100°C, the formation of magic" 7×7 [22] is observed.

The Fe-Si(001) system is similar to the Cr-Si(111) system in the sense that it also exhibits epitaxial growth of metastable FeSi with the CsC1 [23] structure. And the analogy in terms of magic Cr clusters on Si(111) with the 7×7 structure is only qualitative, since on Si(001) clusters can only appear in the form of chains of Fe atoms, which will lead to the 2×1 structure.

Thus, the main problem of this work is to identify and describe the main stages of SWL growth in the Fe-Si(001) system under freezing conditions. The studies carried out made it possible to determine the thickness of the deposited layer at which the SWL−BP transition occurs in this system and to show the role of the atomic environment and collective electronic states in this transition.

2. Simulation and calculation procedure

In this work, although the initial experiments (as mentioned above) were performed in the Cr-Si(111) system, the Fe-Si(001) system was chosen as a test system. This is due to the fact that Fe is close in its chemical reactivity to Cr. In addition, there is a significant amount of data on the Fe-Si(001) system, including experimental results from Plyusnin's group. (see, for example, [14,15,24]). Moreover, this system is of great practical interest, since some of its silicides have unique magnetic and photonic properties and grow epitaxially on Si(001), which is important for the creation of hybrid silicon devices for spintronics and optoelectronics.

The calculation was carried out in a super-cell containing a layer-chain of deposited Fe atoms (gray balls in Fig. 1, 2) and a substrate of Si atoms (black balls in Fig. 1, 2). This super-cell was periodically translated in the plane of the

substrate in two directions along and across the frontal plane of the super-cell, and its size increased step by step after the deposition of adsorbate layers (Fig. 1, 2: from *a* to *f*).

The deposition of a chain of 8 Fe atoms onto the top 5 Si atoms in the super-cell was carried out in steps. In this case, the atoms in the chain were distributed evenly. Step for deposition of Fe atoms was the same – 1.6 ML $(1.2 \cdot 10^{15}$ at/cm$^2)$. The number of Fe steps for deposition increased until the transition from SWL to BP occurred. After each step of deposition, a search was made for the equilibrium state of the system, and then its atomic and electronic structures were calculated. The SWL freezing conditions were met by performing computer simulations of the evolution of the Fe-Si(001) system at zero Kelvin temperature (0 K) under the influence of quantum mechanical forces. At this temperature, this system is transformed, and the Fe atoms found equilibrium states.

In order to test the role of the substrate in the formation of the electronic structure of the film and to reveal the influence of film thickness, an additional experiment was carried out in which a Si substrate in the ⟨001⟩ orientation was matched in lattice constant to the lattice of bulk Fe (Fig. 2). To do this, it was compressed by one third along one axis (in the ⟨011⟩ direction) across the direction of the rows of upper atoms and fitted to the lattice *bcc* Fe. This led to a thickening of the substrate in the frontal and lateral planes (Fig. 2, *a*). Due to this, changes in the electronic structure during the transition from SWL to BP were not affected by the structural rearrangement of the deposited Fe and were due only to the formation of a bulk atomic environment in it.

The calculations were performed using the FHI96spin [25] package, working on the basis of the density functional theory [26,27], as well as within the framework of the pseudo-potential method [28] and a set of plane waves with using one *k*-point of the Brillouin zone (0,0,0). Pseudopotentials were generated using the FHI98PP [29] package, the cutoff energy of the set of plane waves was 50 Ry, and the exchange-correlation interaction was taken into account in the generalized gradient approximation. An atomic system with translational symmetry was specified in a super-cell and during the calculation was translated in three directions with periods $a(X)$, $b(Y)$, $c(Z)$ for two variants of the super-cell: A — Fig. 1 and B — Fig. 2. The values of the parameters $a(X)$, $b(Y)$ and $c(Z)$ of the supercells were equal, respectively: and 20.109 Å.

A Si plate with a (001) surface, which contained four atomic layers of 5 atoms each, was used as a substrate. In this case, the dangling bonds of the lower layer of the plate were saturated with hydrogen atoms (they are shown as purple balls in Figs. 1 and 2). The positions of the lowest Si atoms of the substrate were fixed. The remaining atoms, including Nytrogen ones, could be displaced under the influence of interatomic forces in the process of moving towards an equilibrium position.

First, it be calculated a system with a layer of iron with a thickness of 1 a.d. Fe. And after reaching equilibrium in
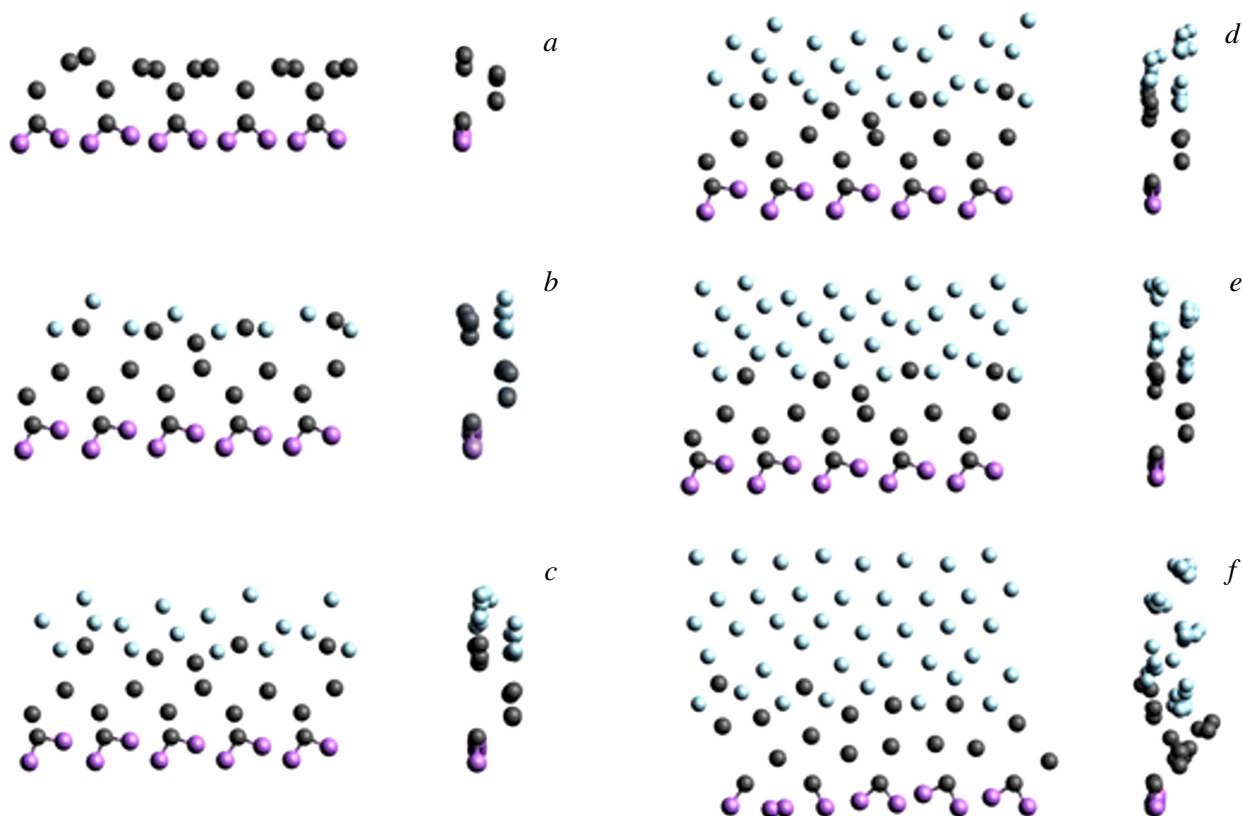
Figure 1. Atomic structure of a normal supercell at various stages of deposition of Fe on Si(001): on fragments *Fx19xEf* is thickness of deposited Fe: 0, 1.6, 3.2, 4.8, 6.4, 8.0 ML respectively. Gray, black and purple balls — these are atoms, respectively: Fe, Si and H.

it, a second layer of the same thickness was applied and so on.... Fe atoms were deposited at a certain distance from the substrate in the form of linear chains in the gap between the upper rows of the (001) Si surface. In mode B, due to the fact that silicon was artificially compressed 1.33 times along one axis (perpendicular to the atomic chains in the direction $\langle 011 \rangle$, the iron atoms in the chain were packed, as in a crystal bcc-Fe.

Equilibrium total energy values, equilibrium atomic configurations, and sets of energy and density of electronic states (DOS) values were obtained. In this case, the DOS levels were bustled using the Gaussian function, which had a half-width of 0.1 eV. In addition, for data comparison, DOS was calculated for bcc-Fe fcc-Fe.

3. Results and discussion

3.1. Change in atomic structure as layers Fe are deposited

Experiment A. As can be seen from Fig. 1, *a, b*, at the first step, a chain of 8 Fe atoms lay on the substrate in the form of a snake consisting of atoms displaced alternately up and down and located in the depressions between the upper atomic rows of Si. As a result, the Fe atoms formed an 2*D*-SWL layer of average composition Fe_2Si_{1+x} ($x = 0.25$), in which the Fe atoms had a 2-fold coordination with the

nearest neighboring Si atoms. In this case, the Fe atoms displaced neighboring Si atoms, formed a lateral bond with them, and left one Si atom (in the middle of the cell) unbound Note that the composition of Fe_5Si_3 is close to the composition of Fe_2Si_{1+x} in the Fe layer (thickness 1.5 ML), obtained in the work [30] by electron beam deposition of Fe on Si(001) at room temperature temperature. This, on the one hand, confirms the result of this modeling, and on the other hand, indicates compliance with the freezing conditions in the work.

On the next 2nd (Fig. 1, *c*), 3rd (Fig. 1, *d*) and 4th (Fig. 1, *e*) steps, the 2nd, 3rd and 4th chains of Fe atoms were also located „snakes" in the middle between the already deposited „snakes". At 3.2 ML, the 1st chain lay more densely over the upper row of Si atoms, forming 2*D*-SWL Fe with 2-fold coordination of atoms. And 3rd and 4th chains at 4.8 and 6.4 ML were formed with underlying layers of 3*D*-SWL Fe, in which the coordination of atoms increased to six and, accordingly, to ten.

In 3*D*-SWL there was already a 3-dimensional environment of a number of Fe atoms by other rows of Fe atoms, as well as coordination typical of bulk phases. According to the arrangement of atoms, as can be seen from the comparison of Fig. 1 and 2 at this step, lattice Fe of this 3*D*-SWL was similar bc-monoclinic: it was compressed in thickness, expanded along the horizontal axis and deformed, forming an inclination of one of the faces to this axis.
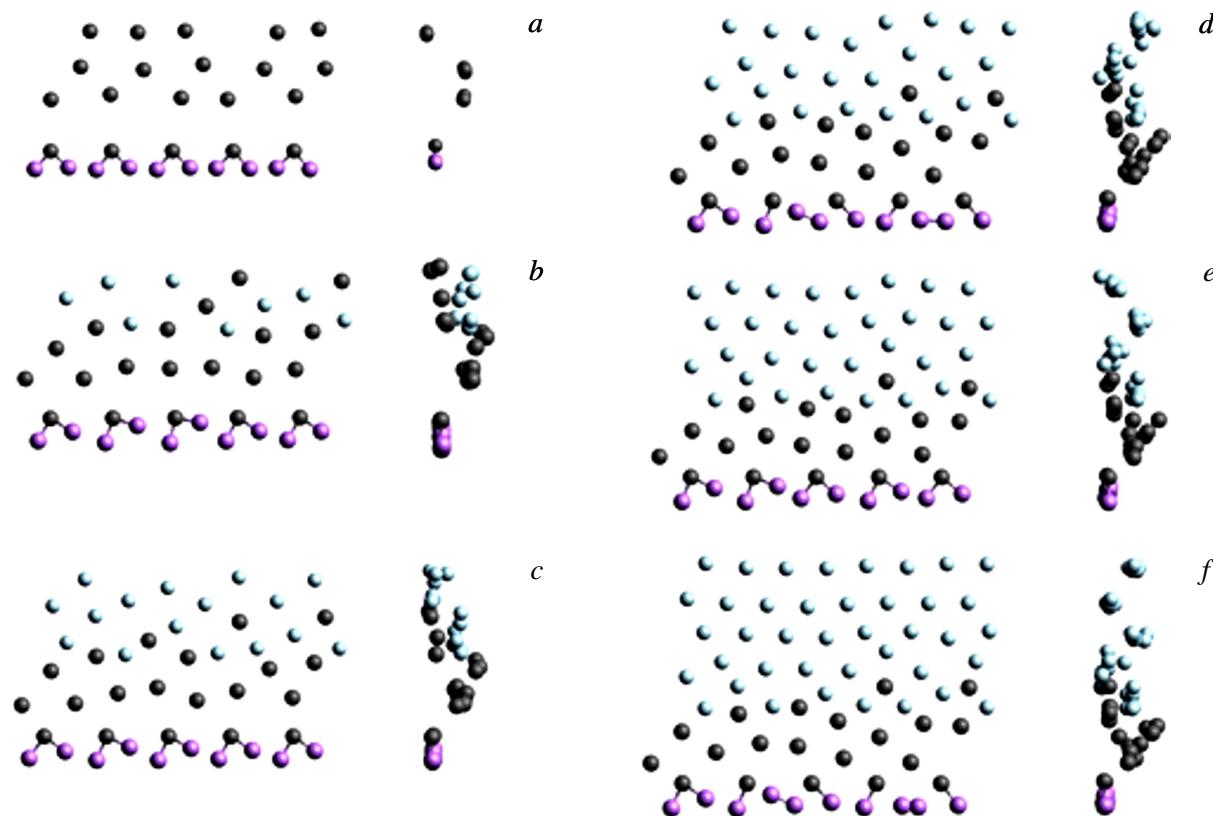
Figure 2. Atomic structure of a compressed super-cell at various stages of Fe deposition on Si(001): on fragments *a−f* is tisthickness of deposited Fe: 0, 1.6, 3.2, 4.8, 6.4, 8.0 ML respectively. Gray, black and purple balls — these are atoms, respectively: Fe, Si and H.

Note that the Fe film with a thickness of 3.2−6.4 ML does not correspond to the FeSi composition obtained by deposition of five ML Fe on Si(001) from a heated Fe [31] filament. It is possible that the high temperature of the filament in the present work provided a high thermal power of the steam, and this, as was shown in the work [32], promotes mixing. In contrast to this, in the work [32], stirring was avoided and a Fe film was obtained due to the reduced temperature of the Fe source (Fe bar wrapped in W wire). A this result is consistent with the result of the present simulation.

At the 5th step (Fig. 1,*f*), the deposition of Fe made the *bc*-monoclinic lattice unstable, and it rearranged itself: it expanded in thickness and straightened out in slope. As a result, an *bc*tetragonal lattice with coordination of 10 atoms was formed, similar at this step to the*bcc* lattice in experiment B, but expanded relative to it in depth (perpendicular to the frontal plane).

In this case, a radical restructuring of the atoms in the Si substrate occurred: they changed the type of packing and moved to the same frontal position as in the case of experiment B, where the substrate was compressed perpendicular to the frontal direction (Fig. 2,*f*). This type of packing of Si atoms most likely corresponds to the high-pressure hexagonal phase of silicon [33], in which the base plane coincides with the front plane, but which is distorted by stresses between the Fe film and the fixed lower Si atoms.

The fact that a stable phase Fe with *bcc* lattice is not yet formed on Si(001) at eight ML is confirmed by the phase diagram of the Fe-Si(001) system given in [34]. At the same time, the study of multilayer Fe/FeSi structures shows that, under the influence of neighboring FeSi layers, there exists a metastable phase Fe [35]. It is possible that the type of packing in the Fe phase formed at eight ML is similar to the packing in this phase (CsCl packing type). Note that studies of the growth of Pb on Si(111) at 150 K also showed that the bulk phase of Pb is formed only starting from ten ML Pb [36]. Note also that the two-stage behavior of the system in this experiment is similar to the two-stage growth of Fe on Si(001) with an epitaxial interlaminar layer CoSi2 [37]. In this case, the Fe lattice underwent tetragonal distortion at the first stage, and at the second stage (in thicker layers) it relaxed to its natural *f cc* lattice.

Experiment B. Then,, frontal compression of the Si(001) substrate, as follows from Fig. 2,*a*, led to its decompression due to the fact that its upper layers changed the type packings in thickness — to a less dense type and broke away from the lower (fixed) layer of Si atoms.

Therefore, as can be seen from Fig. 2,*b*, at the first step, Fe atoms penetrated deeper into the substrate and mixed (in the frontal plane) with the upper two layers of Si, forming the FeSi composition with them. And the lowest of the upper layers of Si increased its composition to seven ones and moved closer to the fixed lowest atoms Si.
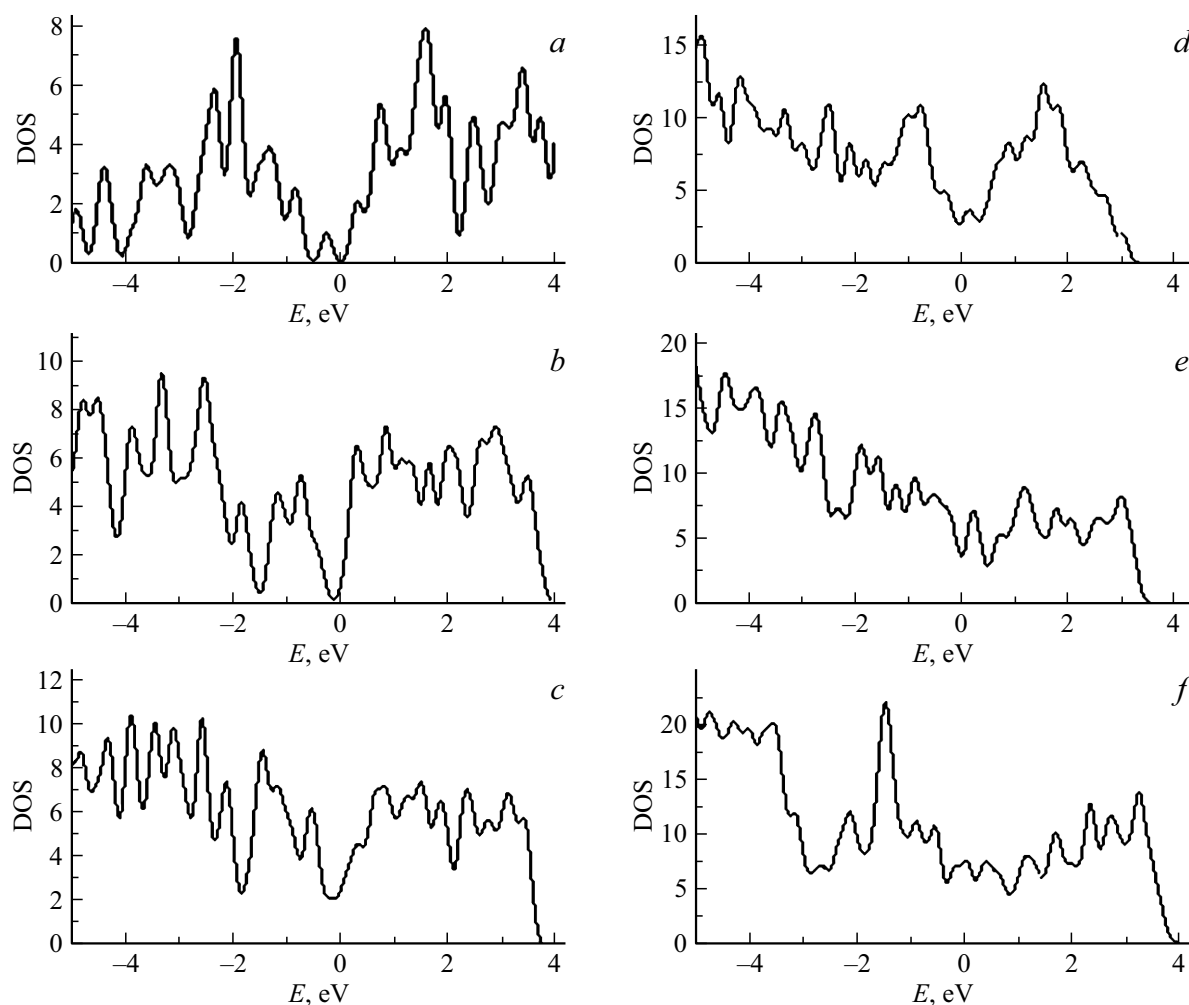
Figure 3. Atomic structure of a normal supercell at various stages of deposition of Fe on Si(001): on fragments *a−f* thickness of deposited Fe: 0, 1.6, 3.2, 4.8, 6.4, 8.0 ML respectively.

Note that in both experiments A and B the silicide composition 2*D*-SWL at the 1st step of deposition (Fig. 1, *b*, 2, *b*) was realized in due to the immersion of Fe in silicon interstices. But in experiment B, mixing occurred to the composition FeSi and at the same time the ordered atom arrangement Fe was lost. Obviously, lattice compression contributed to this and the formation of a disordered mixture FeSi became energetically more favorable.

On the next 2nd (Fig. 2, *c*), 3rd (Fig. 2, *d*), 4th (Fig. 2 , *e*) and 5th (Fig. 2,*f*) steps, the Fe atoms lay down almost as in case A, but less densely and more disordered, forming layer by layer the type of packing of bulk *bcc*-Fe with coordination of 10 atoms. In this case, the intermediate layer 2*D*-SWL FeSi remained unchanged, and the three-dimensional environment of the Fe rows and the compaction of the Si substrate atoms were completed at the 4th step.

At the 5th step (Fig. 2,*f*) the Fe atoms were ordered frontally in rows and an *bcc*-lattice of a stable phase of bulk Fe was formed. In this case, the Si substrate acquired a denser packing of layers in the form of a deformed high-pressure hexagonal phase of Si (see above).

In experiments A (Fig. 1,*f*) and B (Fig. 2,*f*), the Fe and Si lattices formed at this step were similar in the frontal plane, but they turned out to be mirror images of each other. Obviously, this difference is due to the fact that in experiment A, unlike experiment B, a metastable phase was formed. This is evidenced by the fact that the energy of the system at this step in experiment A was on average 1.73 Ry higher than in experiment B.

3.2. Change in atomic structure as layers Fe are deposited

The difference between the DOS structure of Si substrates in experiments A (Fig. 3, *a*) and B (Fig. 4, *a*) was that in experiment B, frontal compression of the Si(001) lattice and its decompression along the thickness (see above) led to the de-hybridization of DOS and the appearance of a pronounced line structure in them.

As can be seen from Figs. 3, *b* and 4, *b*, at the first step, DOS increased along the edges of the valence and free bands, as well as on different sides of the Fermi
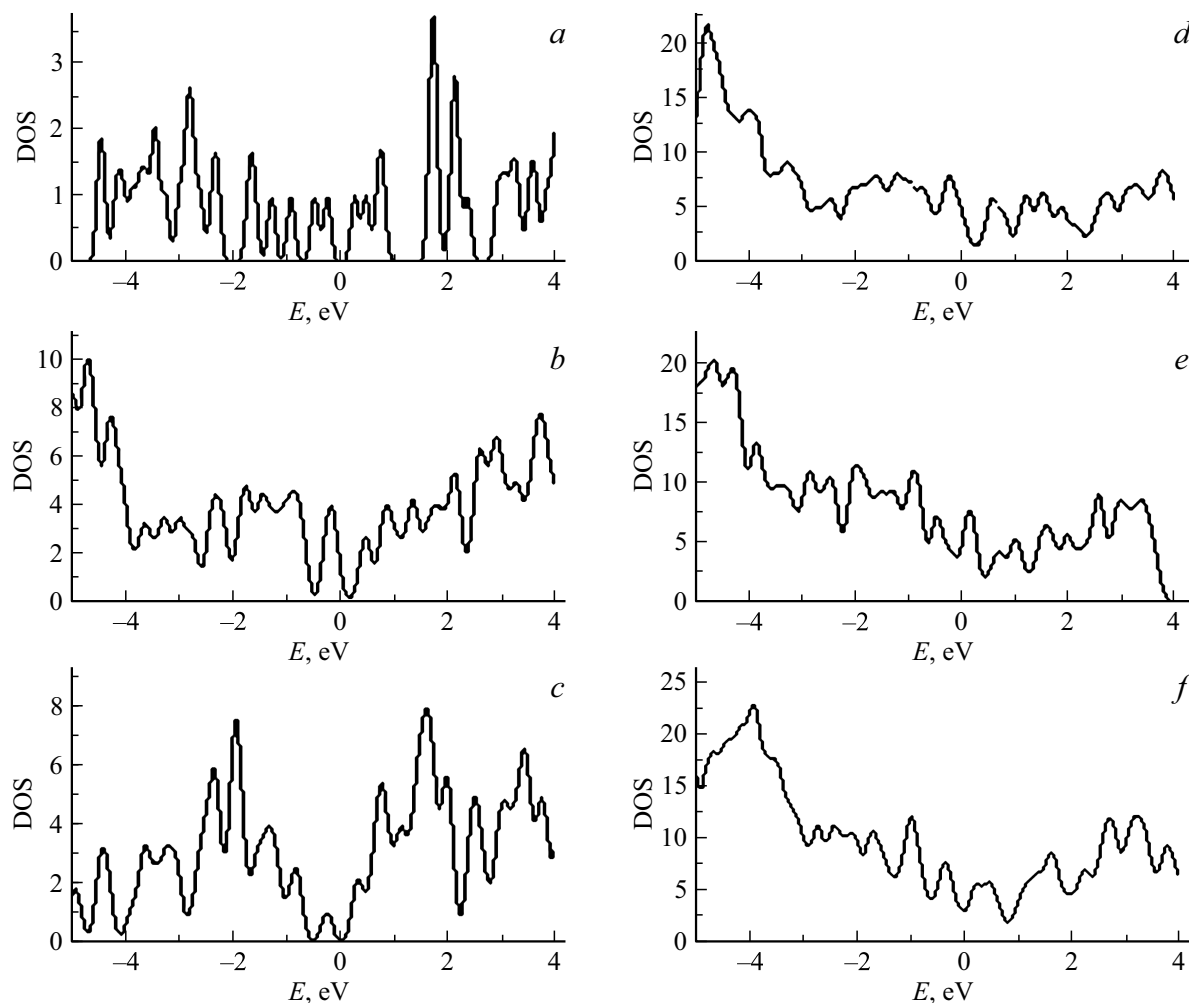
Figure 4. Atomic structure of a normal supercell at various stages of deposition of Fe on Si(001): on fragments $a-f$ is thickness of deposited Fe: 0, 1.6, 3.2, 4.8, 6.4, 8.0 ML respectively.

level. This is due to the formation of binding and antibonding states d-states of metal and sp-states of silicon during their hybridization [1,38] and correlates with the formation of silicide $2D$ solid wetting layers (SWLs) with an average composition Fe_2Si_{1+x} and, accordingly, FeSi(see section 3.1). In experiment B, this led, in addition to eliminating the DOS line structure, to a shift of the DOS minimum beyond the Fermi level. This shift corresponds to the data of the work [39], which shows the electronic structure of FeSi with a DOS minimum located 0.81 eV above the Fermi level.

At the next 2nd, 3rd and 4th steps (respectively, Fig. 3, c, 4, c; 3, d, 4, d; 3, e, 4, e) the contribution of the d states of the metal increased in proportion to the thickness Fe, and the contributions of the hybridized d-and sp- fortunes decreased. In this case, the band gap near the Fermi level disappeared already at the 2nd step, and the silicide electronic structure completely disappeared at the 4th step. This corresponds to the growth of silicide interlayers in the form of $2D$-of SWLs considered above and the growth of SWL on top of them. The differences in the DOS structure

for experiments A (Fig. 3) and B (Fig. 4) at the 1st, 2nd and 3rd steps can be associated with the formation of different types of silicide bonds at the 1st step (Fe_2Si and FeSi).

At the 4th step, as shown by comparison with the electronic structure of fcc- and bcc-Fe and as can be seen from a comparison of Figs. 3 and 4, an electronic structure similar to that for the bulk phase bcc-Fe was formed. Obviously, this happened due to the 10-fold coordination of atoms in the 10-fold coordination of atoms in the $3D$-SWLs (Section 3.1).

Therefore, at the 5th step (Fig. 3, f and 4, $3D$-SWLs Fe became unstable, and a transition to a more stable type of packing Fe occurred (bcc-Fe) with the formation of the corresponding DOS. However, in experiment A, the DOS structure at this step was significantly different from the DOS structure bcc-Fe B in experiment A. This difference was characterized by the presence of a sharp peak, an increased DOS value and a DOS cutoff in the energy range, respectively: from -0.25 to , from to -3.5, and to -5 and from 3.5 to 4 eV. These differences are associated with the formation of bulk phases (BP) Fe: in the experiment A —

metastable BP with the *bc* tetragonal lattice Fe and in the experiment B — stable BP with the *bcc* lattice (which is characterized by a minimum DOS near energy 1 eV).

A comparison of the results obtained in experiment A with data on the growth of Fe on Si(001) under freezing conditions (room temperature of the substrate and low vapor temperature — see [14]) showed their good agreement. In particular, the transition to BP Fe occurred between 7.5 and 15 ML Fe, which corresponds to the range in the present simulation from 6.4 to 8 ML.

Conclusion

Using the method of quantum simulating, it was found that, regardless of the normal (A) or compressed (B) state of the silicon substrate along the $\langle 011 \rangle$ axis, the growth of a solid wetting layer of iron occurs with the formation of an 2*D*-silicide at the first stage. After 2*D*-silicide, 2*D* and 3*D*-wetting layers and then bulk iron phases are sequentially formed. It was found that the bulk phases are preceded by an increase in the coordination of iron atoms in the wetting layer to a value corresponding to the bulk environment in iron, and the formation in it of valence bands similar in structure and electron density to the corresponding zones in the bulk phase of iron. The formation of valence bands enhances the electronic interaction inside the wetting iron layer, as well as between it and the silicon substrate, and creates stress in the film (wetting layer)-substrate system. Relaxation of the latter causes a transformation of this system, which is accompanied by the transition of the wetting layer to a metastable and stable bulk phase for A- and, respectively, B-type substrates, and is also accompanied by the formation of high-pressure silicon phases in these substrates.

Conflict of interest

The authors declare that they have no conflict of interest.

References

[1] J.H. Weaver. Studies *of Silicon-Refractory Metal Interfaces: Photoemission Study of Interface Formation and Compound Nucleation. Final report No AD-A-150075/0/XAB* (Minnesota Univ., Minneapolis, USA, 1984). https://doi.org/10.21236/ada135340

[2] J.H. Weaver. Phys. Today, **39** (1), 24 (1986). https://doi.org/10.1063/1.881062

[3] J.H. Weaver. http://jhweaver.matse.illinois.edu/JHW.pdf

[4] M.V. Gomoyunova, I.I. Pronin. Tech. Phys., **49** (10), 1249 (2004). https://doi.org/10.1134/1.1809696

[5] N.I. Plyusnin, A.V. Kostyuk (red.). *Tverdyy smachivayushchiy sloy* (Bol'shaya rossiyskaya entsiklopediya, M., 2023) (in print)

[6] N.I. Plyusnin. Physics Solid State, **61** (12), 2431 (2019). https://doi.org/10.1134/s1063783419120394

[7] J.A. Venables, G.D.T. Spiller, M. Hanbucken. Reports Progr. Phys., **47** (4), 399 (1984). https://doi.org/10.1088/0034-4885/47/4/002

[8] V.G. Lifshits, N.I. Plyusnin. *Elektronnaya struktura i silitsidoobrazovaniye v tonkikh plenkakh perekhodnykh metallov na kremnii* (Institute of Automation and Control Processes of Far East Scientific Center of the USSR Academy of Sciences, Vladivostok, 1984), preprint № 18, issue 127, 35 p.

[9] V.G. Lifshits, N.I. Plusnin. Phys., Chem. Mechan. Surf., **3**, 2669 (1985).

[10] K. Adamchuk, I.V. Lyubinetsky, A.M. Shikin. Pisma v ZhTF, **12** (17), 1056 (1986) (in Russian).

[11] P.W. Anderson. In: *Elementary Excitations in Solids, Molecules, and Atoms*. Part A (Springer US, Boston, MA, 1974). https://doi.org/10.1007/978-1-4684-2820-9_1

[12] F. Flores, J. Ortega, R. Pérez. Surf. Rev. Lett., **6** (03−04), 411 (1999). https://doi.org/10.1142/s0218625x99000421

[13] J.C. Inkson. J. Phys. C: Solid State Phys., **6** (8), 1350 (1973). https://doi.org/10.1088/0022-3719/6/8/004

[14] N.I. Plyusnin, V.M. Il'yashchenko, S.A. Kitan', S.V. Krylov. J. Surf. Investigation. X-Ray, Synchrotron and Neutron Techniques, **3**, 734 (2009). https://doi.org/10.1134/s1027451009050139

[15] N.I. Plyusnin. Kondensirovannye sredy i mezhfaznye granitsy, **25** (4), 2023 (2021) (in Russian).

[16] H. Brune, K. Kern. Chem. Phys. Solid Surf., **8**, 149 (1997). https://doi.org/10.1016/s1571-0785(97)80008-9

[17] U.K. Köhler, J.E. Demuth, R.J. Hamers. Phys. Rev. Lett., **60** (24), 2499 (1988). https://doi.org/10.1103/physrevlett.60.2499

[18] St. Tosch, H. Neddermeyer. Phys. Rev. Lett., **61** (3), 349 (1988). https://doi.org/10.1103/physrevlett.61.349

[19] V.G. Lifshits, V.G. Zavodinskii, N.I. Plyusnin. Phys., Chem. Mechan. Surf., **2**, 784 (1984).

[20] N.G. Galkin, V.G. Lifshits, N.I. Plyusnin. Poverkhnost. Fizika, khimiya, mekhanika **12**, 50 (1987) (in Russian).

[21] P. Wetzel, C. Pirri, J.C. Peruchetti, D. Bolmont, G. Gewinner. Solid State Commun., **65** (10), 1217 (1988). https://doi.org/10.1016/0038-1098(88)90926-x

[22] O.A. Utas, T.V. Utas, V.G. Kotlyar, A.V. Zotov, A.A. Saranin, V.G. Lifshits. Surf. Sci., **596** (1−3), 53 (2005). https://doi.org/10.1016/j.susc.2005.09.004

[23] H. Von Känel, K.A. Mäder, E. Müller, N. Onda, H. Sirringhaus. Phys. Rev. B, **45** (23), 13807 (1992).

[24] N.I. Plusnin. Tech. Phys., **68** (1), 146 (2023). https://doi.org/10.21883/tp.2023.01.55449.191-22

[25] M. Bockstedte, A. Kley, J. Neugebauer, M. Scheffler. Comp. Phys. Commun., **107** (1−3), 187 (1997). https://doi.org/10.1016/s0010-4655(97)00117-3

[26] P. Hohenberg, W. Kohn. Phys. Rev., **136** (3B), B864 (1964). https://doi.org/10.1103/physrev.136.b864

[27] W. Kohn, L.J. Sham. Phys. Rev., **140** (4A), A1133 (1965). https://doi.org/10.1103/physrev.140.a1133

[28] M.L. Cohen, V. Heine. In: *Solid State Physics*, **24**. Ed. H. Ehrenreich, F. Seitz, D. Turnbull. (Academic Press, NY., 1970), 37. https://doi.org/10.1016/s0081-1947(08)60070-3

[29] M. Fuchs, M. Scheffler. Comp. Phys. Commun., **119** (1), 67 (1999). https://doi.org/10.1016/s0010-4655(98)00201-x

[30] M. Hasegawa, N. Kobayashi, N. Hayashi. Surf. Sci., **357**, 931 (1996). https://doi.org/10.1016/0039-6028(96)00294-4

[31] K. Konuma, J. Vrijmoeth, P.M. Zagwijn, J.W.M. Frenken, E. Vlieg, J.F. van der Veen. J. Appl. Phys., **73** (3), 1104 (1993). https://doi.org/10.1063/1.353273

[32] N.I. Plyusnin, V.M. Il'yashchenko, S.V. Krylov, S.A. Kitan'. Tech. Phys. Lett., **33** (6), 486 (2007). https://doi.org/10.1134/s1063785007060132

[33] L. Fan, D. Yang, D. Li. Materials, **14** (14), 3964 (2021). https://doi.org/10.3390/ma14143964

[34] J. Chrost, J.J. Hinarejos, P. Segovia, E.G. Michel, R. Miranda. Surf. Sci., **371** (2−3), 297 (1997). https://doi.org/10.1016/s0039-6028(96)01013-8

[35] R. Moons, S. Degroote, J. Dekoster, A. Vantomme, G. Langouche. Nucl. Instrum. Methods Phys. Research Section B: Beam Interactions with Materials and Atoms, **136**, 268 (1998). https://doi.org/10.1016/s0168-583x(97)00695-2

[36] Y.F. Zhang, J.F. Jia, Z. Tang, T.Z. Han, X.C. Ma, Q.K. Xue. Surf. Sci., **596** (1−3), L331 (2005). https://doi.org/10.1016/j.susc.2005.09.006

[37] P. Bertoncini, P. Wetzel, D. Berling, G. Gewinner, C. Ulhaq-Bouillet, V. Pierron Bohnes. Phys. Rev. B, **60** (15), 11123 (1999). https://doi.org/10.1016/s0039-6028(00)00180-1

[38] A. Franciosi, J.H. Weaver. Surf. Sci., **132** (1−3), 324 (1983). https://doi.org/10.1016/0039-6028(83)90545-9

[39] H. Wu, P. Kratzer, M. Scheffler. Phys. Rev. B, **72** (14), 144425 (2005). https://doi.org/10.1103/physrevb.72.144425

Translated by V.Prokhorov